

# The Designed Protein M(II)-Gly-Lys-His-Fos(138–211) Specifically Cleaves the AP-1 Binding Site Containing DNA<sup>†</sup>

Catherine Harford,<sup>‡</sup> Suree Narindrasorasak, and Bibudhendra Sarkar\*

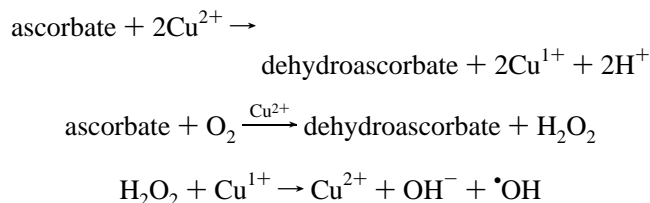
Department of Biochemistry Research, The Hospital for Sick Children, Toronto, Ontario M5G 1X8, Canada, and  
Department of Biochemistry, University of Toronto, Toronto, Ontario M5S 1A8, Canada

Received August 24, 1995; Revised Manuscript Received November 30, 1995<sup>⊗</sup>

**ABSTRACT:** A new specific DNA cleavage protein, Gly-Lys-His-Fos(138–211), was designed, expressed, and characterized. The DNA-binding component of the design uses the basic and leucine zipper regions of the leucine zipper Fos, which are represented by Fos(138–211). The DNA cleavage moiety was provided by the design of the amino-terminal Cu(II)-, Ni(II)-binding site GKH at the amino terminus of Fos(138–211). Binding of Cu(II) or Ni(II) by the protein activates its cleavage ability. The GKH motif was predicted to form a specific amino-terminal Cu(II)-, Ni(II)-binding motif as previously defined [Predki, P. F., Harford, C., Brar, P., & Sarkar, B. (1992) *Biochem. J.* 287, 211–215]. This prediction was verified as the tripeptide, GKH, and the expressed protein, GKH-Fos(138–211), were both shown to be capable of binding Cu(II) and Ni(II). The designed protein upon heterodimerization with Jun(248–334) was shown to bind to and cleave several forms of DNA which contained an AP-1 binding site. The cleavage was shown to be specific. This design demonstrates the versatility of the amino-terminal Cu(II)-, Ni(II)-binding motif and the variety of motifs which can be generated. The site of cleavage by GKH-Fos(138–211) on DNA provides further information regarding the bending of DNA upon binding to Fos–Jun heterodimers.

The amino-terminal Cu(II)-, Ni(II)-binding (ATCUN)<sup>1</sup> motif was first characterized in our laboratory in albumins (Appleton & Sarkar, 1971; Dixon & Sarkar, 1974; Iyer et al., 1978; Glennon & Sarkar, 1982a; Laussac & Sarkar, 1984; Predki et al., 1992; Harford & Sarkar, 1995). Through our studies in the characterization of the ATCUN motif both within albumins and as various tripeptides, we were able to predict that the minimal requirements for such a motif were (1) a free amino terminus, (2) a histidine residue in the third position, and (3) two intervening peptide nitrogens (Predki et al., 1992). The characterization of the metal-binding properties of this motif in albumins enabled us to design and solve the X-ray crystal structure of the minimal motif necessary for the specific binding of Cu(II), Gly-Gly-His (Lau et al., 1974; Camerman et al., 1976). This tripeptide was shown to bind metals and has a metal transport function similar to that of the ATCUN site of albumin (Kruck et al., 1976; Sarkar et al., 1978; Laussac & Sarkar, 1980a,b; Lau & Sarkar, 1981; Glennon & Sarkar, 1982a,b; Glennon et al.,

1983; Tabata & Sarkar, 1985a,b). Further functional studies of this motif were carried out by Pauling and co-workers, who demonstrated that GGH-Cu(II) possessed antitumor activity in the presence of ascorbate (Kimoto et al., 1983). It was also demonstrated that GGH-Cu(II) had DNA- and protein-cleavage capabilities (Chiou, 1983). This reactivity of the motif is due to the strong oxidizing potential of Cu(II) (Shriver et al., 1994). When bound to protein ligands, Cu(II) is much less reactive than when free in solution. However, a significant amount of reactivity still exists. Copper(II) bound to GGH is thought to cleave DNA utilizing the following reaction pathways (Chiou, 1983):



The highly reactive hydroxyl radical ( $\cdot\text{OH}$ ) can react with the DNA backbone and cleave the DNA strand. Therefore, in the presence of ascorbate, Cu(II)-GGH can produce  $\cdot\text{OH}$  which in turn can cleave DNA. Similar reactions involving Cu(II)-GGH with other reducing agents such as DTT and glutathione produce superoxide radical ( $\text{O}_2^-$ ), which is a much less reactive radical species than  $\cdot\text{OH}$  (Chiou, 1983). However, superoxide and  $\text{H}_2\text{O}_2$  combine to produce free hydroxyl radicals:  $\text{H}_2\text{O}_2 + \text{O}_2^- \rightarrow \text{O}_2 + \text{OH}^- + \cdot\text{OH}$  (Haber & Weiss, 1934). Both superoxide anions and hydrogen peroxide are produced *in vivo*. Superoxide anions ( $\text{O}_2^-$ ) are released from hemoglobin-bound  $\text{O}_2$  at a rate of  $10^3$ – $10^6$  molecules per erythrocyte per second (Tonetti et al., 1993). Superoxide dismutase converts superoxide to  $\text{H}_2\text{O}_2$  and  $\text{O}_2$  (Klein et al., 1991; Tonetti et al., 1993).

<sup>†</sup> This work was supported by Grant 003925 from the National Cancer Institute of Canada. C.A.H. was supported by a studentship from the Medical Research Council of Canada.

\* Author to whom correspondence should be addressed at the Research Institute—Biochemistry, The Hospital for Sick Children, 555 University Ave., Toronto, Ontario M5G 1X8, Canada. Tel: (416) 813-5921. Fax: (416) 813-5379.

<sup>‡</sup> Current address: Department of Surgery, Massachusetts General Hospital, Harvard Medical School, Boston, MA 02114.

<sup>⊗</sup> Abstract published in *Advance ACS Abstracts*, February 15, 1996.

<sup>1</sup> Abbreviations: AP-1, activator protein 1; ATCUN motif, amino-terminal Cu(II)-, Ni(II)-binding motif; bp, base pair; BSA, bovine serum albumin; bZIP, basic leucine zipper; DTT, dithiothreitol; GST, glutathione S-transferase; HPLC, high-pressure liquid chromatography; HSC, Hospital for Sick Children; IPTG, isopropyl  $\beta$ -D-thiogalactopyranoside; LB, Luria–Bertani; NP40, Nonidet P40; PBS, phosphate-buffered saline; PCR, polymerase chain reaction; PMSF, phenylmethanesulfonyl fluoride; SDS, sodium dodecyl sulfate; wbFos, weebbug Fos; wbJun, weebbug Jun.

Protein-bound Ni is also able to cleave DNA. When bound to peptides or proteins, the chemistry of Ni is different from free Ni(II). Nickel undergoes redox cycles between Ni(III) and Ni(II) when it is bound to proteins (Klein et al., 1991). Due to these differing redox properties, Ni is unable to produce DNA cleavage in the presence of ascorbate. However, Ni(II)-GGH can produce hydroxyl radicals and superoxide anions in the presence of H<sub>2</sub>O<sub>2</sub> (Torreilles et al., 1990).

The simplest ATCUN motif, GGH, was first used in the design of a DNA cleavage protein by Mack and Dervan in a set of elegant experiments (Mack et al., 1988; Mack & Dervan, 1990, 1992). Subsequently, other groups have used GGH in similar designs (Shullenberger et al., 1993; Nagaoka et al., 1994). On the basis of the definition of the ATCUN motif, it could be predicted that any peptide with (1) a free amino terminus, (2) a histidine residue in the third position, and (3) two intervening peptide nitrogens could form a specific Cu(II)-, Ni(II)-binding protein (Predki et al., 1992; Harford & Sarkar, 1995).

Fos and Jun are two very well characterized leucine zipper proteins. They are oncogenic transcription factors which bind to AP-1 binding sites as dimers [reviewed in Curran (1992)]. The consensus sequence of the AP-1 binding site is TGACTCA. The AP-1 binding site is present in the promoters of many genes. Fos prefers to bind as a heterodimer with Jun to AP-1 binding sites (Patel et al., 1994). Homodimers of Fos are not readily formed. Jun homodimers form easily and bind to the AP-1 binding site on DNA.

Binding of Fos and Jun to DNA causes the DNA to bend. Fos–Jun heterodimers bend DNA in the opposite direction than do Jun–Jun homodimers (Kerppola & Curran, 1991a,b). Bending of DNA by transcription factors provides a mechanism whereby the contacts between those transcription factors and other proteins bound to the DNA can be altered. Therefore, it is likely that the binding of a Fos–Jun heterodimer to DNA may have different effects than the binding of a Jun–Jun homodimer. The kinetics of Fos–Jun association and dissociation in solution are very rapid (Patel et al., 1994). Once a Fos–Jun heterodimer is bound to DNA, however, the release is very slow.

The protein designed here used a novel version of the ATCUN motif, GKH. This motif was introduced at the amino terminus of the basic and leucine zipper regions of Fos. The designed protein was then expressed and purified, and its metal-binding and DNA cleavage abilities were characterized. This design produces an expressible protein which now possesses a metal-binding site where no metal-binding site existed previously.

## DESIGN

The DNA cleavage protein was designed on the basis of the chemistry of Ni and Cu in proteins, the ATCUN motif, and Fos. We have designed the motif peptide, GKH, on the basis of our original design of GGH (Lau et al., 1974; Sarkar et al., 1976; Camerman et al., 1976; Sarkar, 1977).

Several groups of DNA-binding proteins were considered in the designing of this DNA cleavage protein. DNA-binding proteins such as zinc fingers and zinc twists were rejected as these classes of proteins already contain one or more metal-binding domains. It has been shown that these metal-

binding domains may bind other metals including Cu(II) and Ni(II) (Predki & Sarkar, 1992; Nagaoka et al., 1993). Such binding may interfere with binding of metals at the ATCUN motif and/or may result in cleavage of DNA or protein due to Cu(II) or Ni(II) binding at these other metal-binding sites.

Leucine zippers are a well-characterized class of DNA-binding proteins which often bind as heterodimers. In order to produce a dimer which would have only one site with an ATCUN motif, it was necessary to use a leucine zipper protein which prefers to bind as a heterodimer. Fos and Jun are leucine zippers which prefer to bind to AP-1 binding sites on DNA as Fos–Jun heterodimers. The functional domains of Fos are easily demarcated by its amino acid sequence. Therefore, it is relatively easy to design a small motif such as the ATCUN motif close to the amino-terminal end of the DNA-binding region of this protein without disrupting DNA binding. As well, the activation and inhibitory domains of the protein may be removed without significantly affecting DNA binding or dimerization. Fos was chosen because its homodimers do not form as readily as Jun homodimers. Therefore, it would be more likely that only one active protein would be present in each dimer.

It was decided that the design of the DNA cleavage protein would include the placement of an ATCUN motif at the amino-terminal end of the basic and leucine zipper domain of Fos represented by Fos(138–211) (Abate et al., 1990). This segment of Fos contains the histidine which is close to the carboxy-terminal end of the leucine zipper region which has been shown to be important for dimerization (Curran, 1992). The corresponding Jun basic and leucine zipper regions were used as the complementary leucine zipper. These are present in Jun(248–334).

Molecular modeling utilizing the X-ray structure coordinates of Cu(II)-GGH and using the program INSIGHT showed that an ATCUN motif with lysine in the second position should form a structure similar to GGH. The positively charged lysine residue in the second position from the amino terminus should also increase the affinity of the motif for DNA due to electrostatic interactions with the negatively charged phosphate backbone as well as having a higher propensity for  $\alpha$ -helicity upon binding to DNA (Johnson et al., 1994). The basic regions of bZIP proteins are predicted to form an  $\alpha$ -helix in the major groove (Fisher et al., 1992). Therefore, a lysine residue should promote DNA binding on the basis of charge and of secondary structure.

The design of this DNA cleavage protein therefore utilizes the following features: (1) expressibility of the DNA cleavage protein; (2) a leucine zipper heterodimer capable of binding to an AP-1 binding site; (3) an ATCUN motif capable of binding Cu(II) and Ni(II); (4) design of the ATCUN motif onto one-half of the leucine zipper dimer; and (5) a lysine residue within the ATCUN motif which was designed to increase affinity between the motif and the DNA.

## MATERIALS AND METHODS

**Materials.** The p2R vector was a kind gift from P. F. Predki. wbFos and wbJun were kind gifts from T. Curran. pRSETA and TA cloning vectors were obtained from Invitrogen (San Diego, CA). All model tripeptides were synthesized and HPLC purified on C18 columns using an

acetonitrile gradient by the HSC Biotechnology Centre. Protein sequencing was done by the HSC Biotechnology Centre. All oligonucleotides were synthesized by the HSC Biotechnology Centre and purified by C18 SepPak using acetonitrile gradients. Hydrogen peroxide was obtained from BDH (Toronto, Canada). Ascorbic acid was obtained from Sigma (St. Louis, MO). Monoperoxyphthalic acid was obtained from Aldrich (Milwaukee, WI). Copper chloride and nickel chloride were obtained from Fisher (Toronto, Canada).

*Expression of GKH-Fos(138–211) and Jun(248–334).* The sequence of the designed protein, GKH-Fos(138–211), is **GKH**RRIRRRERNKMAAAKCRNRRRELTDTLQAET-DQLEDEKSALQTEIANLLKEKEKLEFILAA-HRPACKIPNDLG, showing the ATCUN motif (bold), DNA-binding domain (underlined), and leucine zipper domain (italics).

The expression vectors for the DNA-binding and leucine zipper domains of GKH-Fos(138–211) were constructed. The primers to produce the template for the coding sequences for GKH-Fos(138–211) were as follows: coding strand primer, 5' GCGCCATGGGCAAGCATAAACGTCGCATC; noncoding strand primer, 5' CGCGCGGATCCCTAACCCAGGTC. These primers contained a *NcoI* site in the leading sequence and a *BamHI* site following the stop codon. The coding sequences were generated by PCR using *wbFos* as a template. The PCR products were ligated to the TA cloning vector. The resulting plasmids were amplified in *Escherichia coli* strain InVαF, and the coding sequences were cut with *NcoI* and *BamHI* and cloned into the *NcoI* and *BamHI* sites of expression vector p2R.

The expression vector for the DNA-binding domain of Jun, Jun(248–334), was constructed similarly to the construction of Fos(138–211) using *wbJun* as a template. The primers used were as follows: coding strand primer, 5' GCGCGCGCATGGGCATCGACATGGAGTC; noncoding strand primer, 5' GCGCGCGCGGATCCTTAAACGTTTGCAACTG. The expression of Jun(248–334) was significantly less than the expression of GKH-Fos(138–211) using this method. Both GKH-Fos(138–211) and Jun(248–334) were expressed in *E. coli* strain BL21(DE3)pLysS. Alternatively, Jun(248–334) was expressed as a GST fusion protein in pGEX-4T-2 plasmid (Pharmacia Biotech, Montreal, Canada). By using the same primers that were used to clone into p2R plasmid, the PCR product was first cloned into the TA-PCR vector. The resulting plasmid was cut with *EcoRI*, and the insert was cloned into pGEX-4T-2 at *EcoRI* restriction sites. The fusion protein, after cleavage by thrombin, produced Jun(248–334) with 12 extra amino acids at the amino terminus. The resulting sequence was GSPGIRLARAMG-Jun(248–334).

*Purification of GKH-Fos(138–211) and Jun(248–334).* *E. coli* were harvested from 1 L of LB media after 3 h of induction with IPTG by centrifugation at 5000 rpm for 5 min at 4 °C. The cells were resuspended in 40 mL of buffer containing 50 mM Tris, pH 7.5, 1 mM EDTA, 5 mM DTT, 0.5 M NaCl, 2 mM PMSF, 0.5% deoxycholate, 0.1 mg/mL lysozyme, and 10% glycerol. The cell suspension was stored at –20 °C overnight. Thereafter, the cell suspension was thawed and centrifuged at 40 000 rpm for 40 min. The supernatant was transferred into a fresh tube, and a solution of poly(ethylenimine) was added to a final concentration of 0.2%. This mixture was centrifuged at 40 000 rpm for 30

min. The supernatant was dialyzed against 25 mM phosphate buffer, pH 7.5, containing 1 mM DTT and 10% glycerol. The pellet obtained by centrifugation of the cell suspension contained the majority of the expressed protein. This was extracted with 40 mL of 6 M urea containing 25 mM phosphate buffer, pH 7.5, and 1 mM DTT. The mixture was centrifuged at 40 000 rpm for 30 min, and the supernatant was dialyzed against 25 mM phosphate buffer, pH 7.5, containing 1 mM DTT and 10% glycerol.

The protein from the dialyzed soluble fraction or urea extract was purified on a cation-exchange resin, Bio-Rex 70, 200–400 mesh, equilibrated with 25 mM phosphate buffer, pH 7.5, containing 1 mM DTT and 10% glycerol. The protein was eluted by stepwise gradient increases of NaCl concentration in the buffer. GKH-Fos(138–211) was eluted between 0.5 and 1.0 M NaCl with the majority of the protein which had apparent >90% purity eluting at 0.7 M. The relative purity of the proteins was determined on a 15% SDS–PAGE which was run at 125V for 1.5 h and stained with Coomassie blue dye. Fractions containing >90% pure protein were dialyzed against 25 mM phosphate buffer, pH 7.5, 1 mM DTT, 100 mM NaCl, and 10% glycerol before testing for DNA-binding activity (Xanthoudakis & Curran, 1992). Jun(248–334) was eluted between 0.5 and 1.0 M NaCl, but with only approximately 25% purity. These fractions were dialyzed against 25 mM phosphate buffer, pH 7.5, 1 mM DTT, 100 mM NaCl, and 10% glycerol. The GST-Jun(248–334) was overexpressed in *E. coli* strain BL21(DE3) within inclusion bodies. The insoluble pellet was dissolved in 8 M urea containing 25 mM phosphate buffer, pH 7.5, and 1 mM DTT. The protein was refolded by dialyzing against phosphate-buffered saline (PBS) plus 1 mM DTT. The protein was purified by passing through a glutathione–Sephacrose column (Pharmacia Biotech, Montreal, Canada) according to the supplier's protocol. Both the GST-fused protein and the thrombin-cleaved product GSPGIRLARAMG-Jun(248–334) were able to form heterodimers with GKH-Fos(138–211). Jun(248–334) was used in the plasmid cleavage experiments. GSPGIRLARAMG-Jun(248–334) was used in the 1900 and 100 bp cleavage experiments. GSPGIRLARAMG-Jun(248–334) was approximately 90% pure.

*Visible Spectra.* The visible absorption spectra of the Cu(II)-GKH, Ni(II)-GKH, and Cu(II)-GKH-Fos(138–211) complexes were obtained on a Hitachi U-3210 spectrophotometer. The Cu(II)-GKH and Ni(II)-GKH spectra were determined at 3.3 mM in 0.15 M NaCl at 25 °C. Each of these spectra was obtained as a difference spectrum with the tripeptide in the presence of 1 equiv of Cu(II) or Ni(II), using as a reference the appropriate peptide in the absence of metal at the same pH. The absorption spectrum of Cu(II)-GKH-Fos(138–211) was determined at  $6 \times 10^{-4}$  M at 12 °C in 0.5 M NaCl in a 1 cm path length. Water was used as a reference.

*Mobility Shift Assays.* The DNA used in the mobility shift assays was 5' GATCCCGTGACTCAGCGCGCATCGT-GACTCAGCGCGCA 3' GGCAGTGAAGTCGCGCGTAGCACTGAGTCGCGCGTTTCA. The AP-1 binding sites are underlined. Although the DNA used in the mobility shift assays has two AP-1 binding sites, it has been demonstrated that this does not affect binding of Fos and Jun (Hai & Curran, 1991). The DNA was labeled with <sup>32</sup>P using [<sup>32</sup>P]-ATP and phosphonucleotide kinase. The DNA was purified

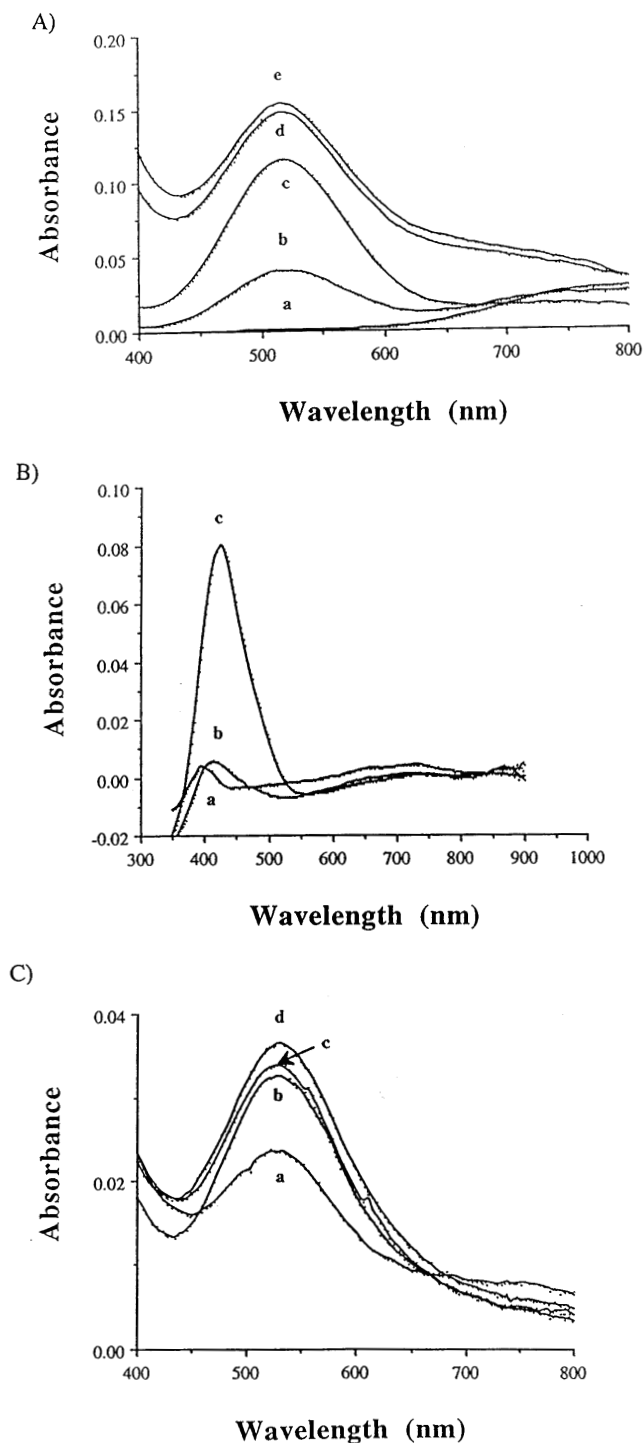


FIGURE 1: Visible spectra. (A) GKH-Cu(II). The spectra were measured at pH 3.87 (a), pH 4.67 (b), pH 6.20 (c), pH 7.55 (d), and pH 9.26 (e). (B) GKH-Ni(II) visible spectra. The spectra were measured at pH 4.53 (a), pH 5.98 (b) and pH 6.71 (c). (C) Cu(II)-GKH-Fos(138-211) visible spectra. The spectra were measured at pH 4.83 (a), pH 6.66 (b), pH 7.48 (c), and pH 9.40 (d).

on a 20% nondenaturing polyacrylamide gel prior to use. Mobility shift assays were run on a native 5.4% polyacrylamide gel in 6.8 mM Tris and 40 mM acetate, pH 7.9, buffer. The gel was prerun at 100 V for 1.5 h. Samples were added to an equal volume of 2× buffer which consisted of 20 mM Tris, pH 7.5, 10 mM DTT, 10 mM MgCl<sub>2</sub>, 100 mM NaCl, 2 mg/mL BSA, 0.2% NP40, and 20% glycerol. The protein mixture was equilibrated for 15 min prior to addition of DNA. The DNA-protein mixture was incubated

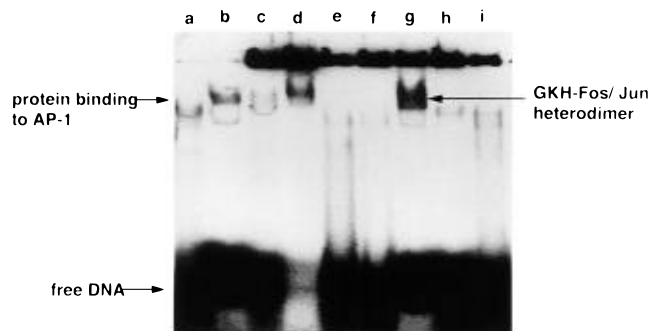


FIGURE 2: Mobility shift assay of GKH-Fos(138-211), Fos(138-211), and Jun(248-334). The oligonucleotide used in the mobility shift assay was 5' TCGACGTGACTCAGCGCGCATCGTGACTCAGCGCGC 3' AGCTGCACTGAGTCGCGCGTAGCACTGAGTTCGCGCGC. Lanes: (a) Fos(138-211), (b) GKH-Fos(138-211), (c) Jun(248-334), (d) Fos(138-211) + Jun(248-334), (e) Fos(138-211) + Jun(248-334) + 100× cold AP-1, (f) Fos(138-211) + Jun(248-334) + 200× cold AP-1, (g) GKH-Fos(138-211) + Jun(248-334), (h) GKH-Fos(138-211) + Jun(248-334) + 100× cold AP-1, (i) GKH-Fos(138-211) + Jun(248-334) + 200× cold AP-1. (AP-1 refers to the AP-1 binding site containing DNA.)

for 15 min at room temperature prior to loading of the gel. The gel was run at 150 V with equilibration of buffers for 1 h, then dried, and exposed to Kodak X-OMAT film overnight with an intensifying screen.

**DNA Cleavage.** Plasmid DNA for cleavage was produced by inserting a 38 bp fragment containing AP-1 binding sites between the *Bam*HI and *Hind*III restriction sites into pRSETA. A 1900 bp fragment of DNA was generated by digesting the same plasmid with restriction enzyme *Nci*I and purifying the 1900 bp fragment by agarose gel electrophoresis. Both the plasmid DNA and the 1900 bp linear DNA were cleaved by the designed protein in the same manner. The GKH-Fos(138-211) protein and equimolar Cu(II) or Ni(II) were first allowed to equilibrate in 0.5 M NaCl for 45 min. The following reagents were added: 10 μL of 5× buffer (50 mM Tris, pH 7.5, 25 mM DTT, 25 mM MgCl<sub>2</sub>, 250 mM NaCl, 0.5% NP40, and 50% glycerol), enough H<sub>2</sub>O to make total volume to 50 μL, and Jun(248-334). Due to DNase contamination in Jun(248-334) preparations where Jun(248-334) was not expressed as the GST fusion protein, the protein mixture was heated to 100 °C for 10 min prior to DNA addition in those mixtures where that Jun(248-334) was used. This step was not necessary when Jun(248-334) was expressed as a GST fusion protein. The protein mixture was allowed to equilibrate at room temperature for 15 min. DNA and monoperoxyphthalic acid or H<sub>2</sub>O<sub>2</sub>/ascorbic acid (equimolar to the metal) were then added to all samples. Concentrations of protein and DNA are given in the figure legends. Controls were carried out using free metal or protein without metal instead of M(II)-GKH-Fos(138-211). The DNA-protein mixture was equilibrated at 37 °C for periods of time as indicated in the figure legends. After incubation, equal aliquots of sample were made 0.4% in SDS. Samples were loaded on a 1% agarose gel in 0.05% ethidium bromide, electrophoresed at 100 V for 1 h, and visualized with UV light.

Specificity of cleavage was determined by a reaction with a 100 bp fragment of the AP-1 binding site containing DNA. Cleavage reactions were carried out in a total volume of 25 μL in the same manner as cleavages with the larger fragments

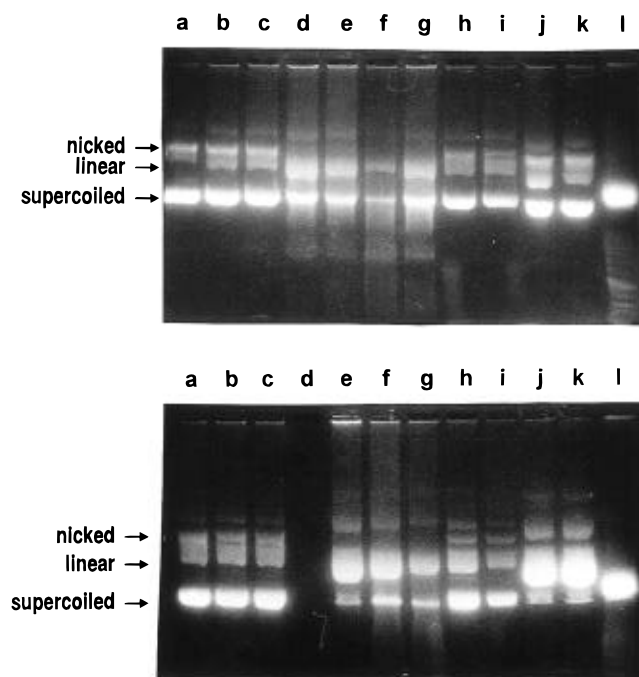


FIGURE 3: Cleavage of supercoiled DNA. (A, top) Supercoiled pRSETA-AP-1 plasmid DNA cleavage in the presence or absence of Ni. Samples were incubated with monoperoxyphthalic acid (20  $\mu$ M) for 17 h at 37  $^{\circ}$ C. The pRSETA-AP-1 concentration was 0.35  $\mu$ M. Lanes (a) AP-1 DNA; (b and c) AP-1 DNA + GKH-Fos(138–211) (20  $\mu$ M); (d and e) AP-1 DNA + Ni(II)-GKH-Fos(138–211) (20  $\mu$ M); (f and g) AP-1 DNA + Ni(II)-GKH-Fos(138–211) (20  $\mu$ M) + Jun(248–334) (4  $\mu$ M); (h and i) AP-1 DNA + GKH-Fos(138–211) (20  $\mu$ M) + Jun(248–334) (4  $\mu$ M); (j and k) AP-1 DNA + Ni(II) (20  $\mu$ M). (AP-1 DNA refers to the AP-1 binding site containing DNA.) (B, bottom) Supercoiled pRSETA plasmid DNA cleavage in the presence or absence of Cu(II). Samples were incubated with monoperoxyphthalic acid (20  $\mu$ M) for 23 h at 37  $^{\circ}$ C. The pRSETA-AP-1 DNA concentration was 0.17  $\mu$ M. Lanes: (a) AP-1 DNA; (b and c) AP-1 DNA + GKH-Fos(138–211) (20  $\mu$ M); (d) no sample; (e) AP-1 DNA + Cu(II)-GKH-Fos(138–211) (20  $\mu$ M); (f and g) AP-1 DNA + Cu(II)-GKH-Fos(138–211) (20  $\mu$ M) + Jun(248–334) (4  $\mu$ M); (h and i) AP-1 DNA + GKH-Fos(138–211) (20  $\mu$ M) + Jun(248–334) (4  $\mu$ M); (j and k) AP-1 DNA + Cu(II) (20  $\mu$ M); (l) 4000 bp DNA marker. (AP-1 DNA refers to the AP-1 binding site containing DNA.)

with the following exceptions: The DNA was 5' end labeled with approximately 20 000 cpm of  $^{32}$ P on one strand of a 100 bp fragment of synthetic DNA containing one AP-1 binding site. One microgram of poly(dIdC)•poly(dIdC) was added to the mixture. After incubation of 20 h was completed, the reactions were stopped by addition of SDS to a final concentration of 0.4%. The DNA was extracted with an equal volume of phenol:chloroform (1:1). Aliquots of the aqueous phase were mixed with equal volumes of gel loading dye. DNA cleavage products were analyzed on a 20% 1:20 cross-linked denaturing polyacrylamide gel electrophoresis followed by autoradiography.

## RESULTS

The proteins were expressed using p2R and purified. Peptide sequencing of the first five residues of the expressed protein demonstrated that the sequence was GKHKR as designed. Visible spectra of the tripeptide, GKH, and of GKH-Fos(138–211) demonstrated that the absorption maxima for GKH-Cu(II), GKH-Ni(II), and Cu(II)-GKH-

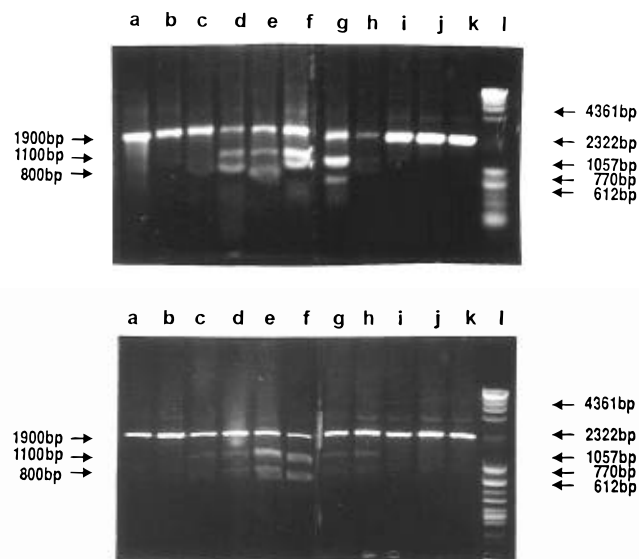


FIGURE 4: Cleavage of 1900 bp DNA. (A, top) Cleavage by Ni(II)-GKH-Fos(138–211) and monoperoxyphthalic acid. Samples were incubated with monoperoxyphthalic acid (20  $\mu$ M) for 18 h at 37  $^{\circ}$ C. The 1900 bp DNA concentration was 0.057  $\mu$ M. Lanes: (a) AP-1 DNA; (b and c) AP-1 DNA + GKH-Fos(138–211) (20  $\mu$ M); (d and e) AP-1 DNA + Ni(II)-GKH-Fos(138–211) (20  $\mu$ M); (f and g) AP-1 DNA + Ni(II)-GKH-Fos(138–211) (20  $\mu$ M) + GSPGIRLARMG-Jun(248–334) (4  $\mu$ M); (h and i) AP-1 DNA + GKH-Fos(138–211) (20  $\mu$ M) + GSPGIRLARMG-Jun(248–334) (4  $\mu$ M); (j and k) AP-1 DNA + Ni(II) (20  $\mu$ M); (l) DNA markers. (AP-1 DNA refers to the AP-1 binding site containing DNA.) (B, bottom) Cleavage by Cu(II)-GKH-Fos(138–211) and monoperoxyphthalic acid. Samples were incubated with monoperoxyphthalic acid (20  $\mu$ M) for 18 h at 37  $^{\circ}$ C. The 1900 bp DNA concentration was 0.057  $\mu$ M. Lanes: (a) and b) AP-1 DNA + GKH-Fos(138–211) (20  $\mu$ M); (c and d) AP-1 DNA + Cu(II)-GKH-Fos(138–211) (20  $\mu$ M); (e and f) AP-1 DNA + Cu(II)-GKH-Fos(138–211) + GSPGIRLARMG-Jun(248–334) (4  $\mu$ M); (g and h) AP-1 DNA + GKH-Fos(138–211) (20  $\mu$ M) + GSPGIRLARMG-Jun(248–334) (4  $\mu$ M); (i and j) AP-1 DNA + Cu(II) (20  $\mu$ M); (k) AP-1 DNA; (l) DNA markers. (AP-1 DNA refers to the AP-1 binding site containing DNA.)

Fos(138–211) were 522, 424, and 520 nm, respectively. These maxima were reached at relatively low pH and maintained through a wide range of pH (Figure 1). This indicates that the tripeptide and the designed protein both bound Cu(II) and Ni(II) specifically, similar to other ATCUN motifs (Predki et al., 1992). GKH-Fos(138–211) was shown to bind to DNA containing an AP-1 binding site as both a homo- and heterodimer with Jun(248–334) (Figure 2). Expression of Jun as a GST fusion protein did not affect the ability of Fos to dimerize with it (data not shown).

DNA cleavage experiments were carried out with several forms of the AP-1 binding site containing DNA. These include supercoiled DNA, a 1900 bp fragment of DNA, and a 100 bp fragment of DNA (Figures 3, 4, and 5). Controls in lanes a of each gel in Figure 3 show that most of the plasmid DNA is in the supercoiled form (Figure 3A,B). A small amount of DNA is in the nicked form. In the absence of metal (lanes b, c, h, and i), little or no DNA is cleaved. In the presence of M(II)-GKH-Fos(138–211), cleavage of the DNA is produced (lanes d, e, f, and g). This is demonstrated in the experiments where plasmid DNA was used by the disappearance of supercoiled DNA and the appearance of linear DNA. Comparison of lanes b and c with lanes d and e and similarly lanes f and g with h and i demonstrates that metal is required for the cleavage. Com-

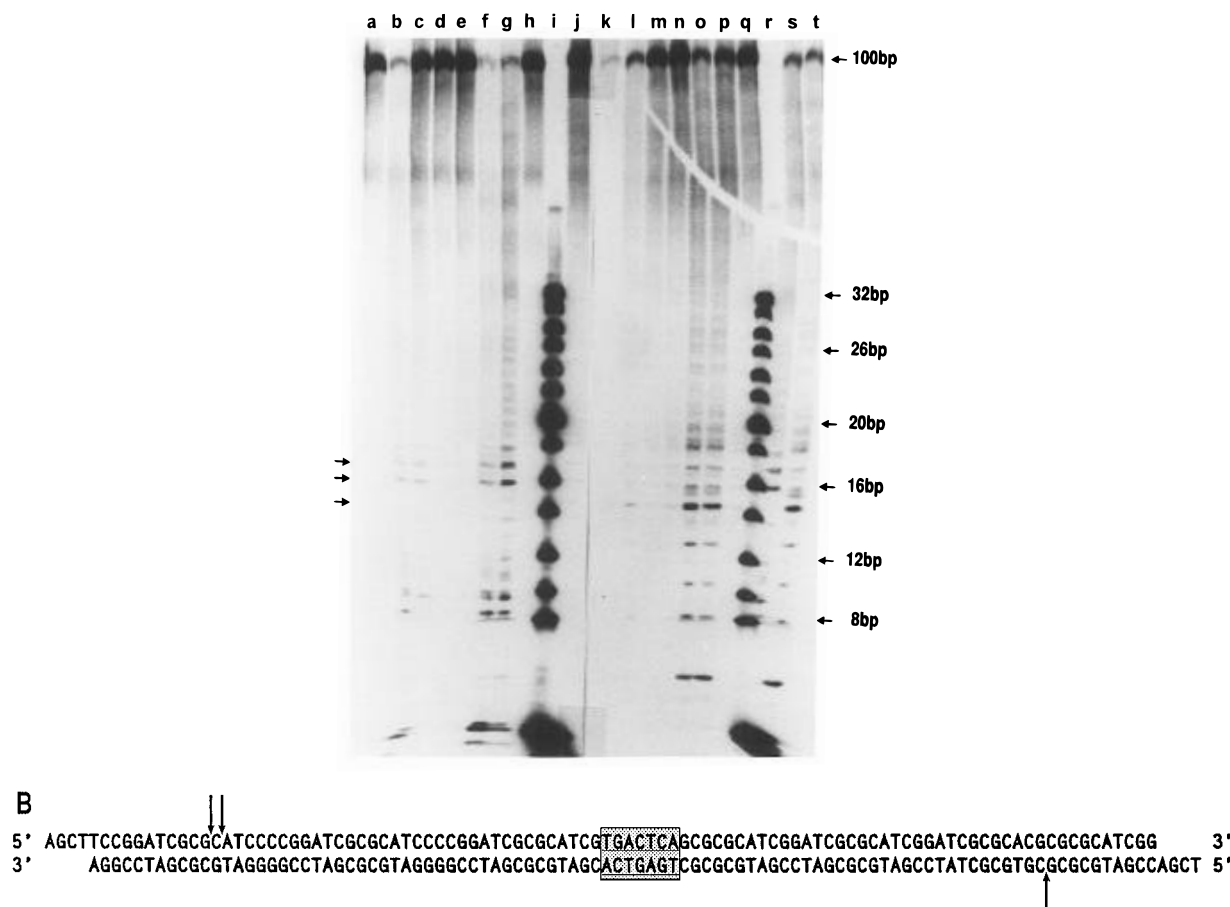


FIGURE 5: Cleavage of 100 bp DNA. (A, top) Cleavage by Cu(II)-GKH-Fos(138–211) in the presence of ascorbate and  $H_2O_2$ . The concentration of GKH-Fos(138–211) was  $7 \mu M$ . The concentration of GSPGIRLARMG-Jun(248–334) was  $1 \mu M$ . The concentrations of ascorbate,  $H_2O_2$ , and Cu(II) were  $7 \mu M$ . Lanes: (a) 5' end-labeled AP-1a (TGACTCA) ( $a^*$ ); (b) GKH-Fos(138–211) +  $a^*$ ; (c) Cu(II)-GKH-Fos(138–211) +  $a^*$ ; (d) GSPGIRLARMG-Jun(248–334) +  $a^*$ ; (e) Cu(II) + GSPGIRLARMG-Jun(248–334) +  $a^*$ ; (f) GKH-Fos(138–211) + GSPGIRLARMG-Jun(248–334) +  $a^*$ ; (g) Cu(II)-GKH-Fos(138–211) + GSPGIRLARMG-Jun(248–334) +  $a^*$ ; (h) Cu(II) +  $a^*$ ; (i) markers; (j) 5' end-labeled AP-1b (TGAGTCA) ( $b^*$ ); (k) GKH-Fos(138–211) +  $b^*$ ; (l) Cu(II)-GKH-Fos(138–211) +  $b^*$ ; (m) GSPGIRLARMG-Jun(248–334) +  $b^*$ ; (n) Cu(II) + GSPGIRLARMG-Jun(248–334) +  $b^*$ ; (o) GKH-Fos(138–211) + GSPGIRLARMG-Jun(248–334) +  $b^*$ ; (p) Cu(II)-GKH-Fos(138–211) + GSPGIRLARMG-Jun(248–334) +  $b^*$ ; (q) Cu(II) +  $b^*$ ; (r) markers; (s) Cu(II)-GKH-Fos(138–211) + GSPGIRLARMG-Jun(248–334) +  $a^*$ ; (t) Cu(II)-GKH-Fos + GSPGIRLARMG-Jun(248–334) +  $b^*$ . The top two arrows on the left-hand side indicate cleavage products of the  $a^*$  strand, and the bottom arrow indicates the cleavage product of the  $b^*$  strand. (B) Sites of cleavage.

parison of lanes d and e with lanes f and g demonstrates that addition of Jun(248–334) increased the amount of cleavage. Shorter incubation times resulted in less cleavage (data not shown). The supercoiled experiments demonstrate that Ni(II)-GKH-Fos(138–211) and Cu(II)-GKH-Fos(138–211) are able to cleave DNA in the presence of monoperoxyphthalic acid. This cleavage is more pronounced when the protein is bound to DNA as a heterodimer with Jun(248–334). As the affinity of the GKH-Fos(138–211)-Jun(248–334) heterodimer for the DNA is greater than that of the GKH-Fos(138–211) homodimer, this result is to be expected. The 1900 bp fragment is cleaved by GKH-Fos(138–211) which has either Cu(II) or Ni(II) bound in the presence of monoperoxyphthalic acid. These reactions show the production of two fragments of approximate sizes 800 and 1100 bp, corresponding to the two halves of the DNA on either side of the AP-1 binding site in the 1900 bp fragment (Figure 4). Figure 3B, lanes j and k, demonstrates that Cu(II) is able to cleave DNA alone. Nickel(II) is less able to cleave DNA in the absence of protein (Figure 3A). These results are due to the differing chemistry of Cu(II) and Ni(II) when free and when protein bound. Free Cu(II)

is highly oxidizing. This reactivity is dampened when the metal is bound to proteins. Therefore, the free Cu(II) is able to cleave the supercoiled DNA significantly (Figure 3B), but this cleavage is not specific (Figure 5A) as opposed to the specific but dampened cleavage by Cu(II)-GKH-Fos(138–211)-Jun(248–334). Nickel, however, has a different chemistry. When protein bound, Ni undergoes redox cycles between Ni(II) and Ni(III) which enables it to have higher oxidizing potential and thus greater DNA cleavage potential than free Ni(II) (Klein et al., 1991).

A sequencing gel which separated the cleavage products of the reaction of Cu(II)-GKH-Fos(138–211) in the presence of ascorbate with 100 bp DNA demonstrates the specificity of the reaction (Figure 5A). The DNA was cleaved in a very narrow range. The cleavage site was 34 and 35 bp 5' from the AP-1 binding site on the " $a$ " strand where the AP-1 binding site was TGACTCA. On the opposite strand " $b$ " where the AP-1 binding site sequence was TGAGTCA, the site of cleavage was 33 bp upstream from the binding site (Figure 5B). Cleavage with Ni(II)-GKH-Fos(138–211) in the presence of monoperoxyphthalic acid showed identical results (data not shown).

## DISCUSSION

We were able to express GKH-Fos(138–211) and GSP-GIRLARAMG-Jun(248–334) in very high yield as well as >95% purity. The binding of GKH-Fos(138–211) and the two Jun constructs to DNA sequences containing AP-1 binding sites was shown to mimic the binding of native c-Fos and c-Jun basic and leucine zipper regions (Figure 2). Therefore, the design of GKH at the amino terminus of Fos(138–211) does not appear to affect dimerization with Jun(248–334) or binding of the dimers to DNA.

*GKH-Fos(138–211) Binds Cu(II) and Ni(II) Specifically.* The lysine residue in the second position of the motif has been demonstrated not to interfere with metal binding in the ATCUN motif. This is despite the  $\epsilon$ -amino group of the side chain which could have displaced the metal atom from its square planar binding site within the motif by charge interference or steric hindrance. These results give further support to the definition of the ATCUN motif and the prediction that the identity of the first two residues in the motif do not make a significant difference in the metal binding of the motif, assuming that the other requirements of the motif are met (Predki et al., 1992; Harford & Sarkar, 1995). Therefore, the motif should be formed with any of the usual 20 amino acid residues in the first two positions, except for proline.

*DNA Cleavage.* The rate of DNA cleavage was relatively slow. GKH-Fos(138–211) and Jun(248–334) were present in excess over the DNA. However, each reaction took several hours to approach completion. Shorter time periods (3 h or less) did not demonstrate significant cleavage of the DNA. This is most likely due to the rapid dissociation of Fos–Jun heterodimers prior to binding to DNA (Patel et al., 1994). Proteins with faster binding to DNA would be expected to show faster cleavage.

Both monoperoxyphthalic acid and the hydrogen peroxide/ascorbate system were shown to be capable of catalyzing the cleavage by Cu(II) or Ni(II) (Figures 3, 4, and 5). The cleavage in each case was shown to be single stranded, indicating that the interaction between the cleavage motif and the DNA was very specific. As well, the radicals generated by the reactions are likely nondiffusible and modify the deoxyribose moiety. Therefore, only single-stranded cleavage occurs.

*Implications of Cleavage for Fos–DNA Interactions.* The X-ray crystal structure of c-Fos and c-Jun binding to the AP-1 binding site has recently been published (Glover & Harrison, 1995). This structure showed Fos(139–200) and Jun(263–324) binding to a 20 bp segment of DNA containing an AP-1 binding site. The closest residue to contact DNA in our motif is Asn147, which is 10 residues from the ATCUN motif in our designed protein. Our cleavage results indicate that the amino terminus of GKH-Fos(138–211) is only bound at the 5' end of the AP-1 binding site. As well, depending upon whether the site is TGAGTCA or TGACTCA, the orientation of GKH-Fos(138–211) to the DNA is slightly altered, as indicated by the slightly different sites of cleavage. This is also consistent with the crystal structure which showed a 10° difference in the orientation of the coiled coil relative to the DNA when the Fos–Jun complex was bound to one strand versus the other (Glover & Harrison, 1995).

These studies give further information to the orientation of Fos(138–211) on DNA. The lack of intervening cuts

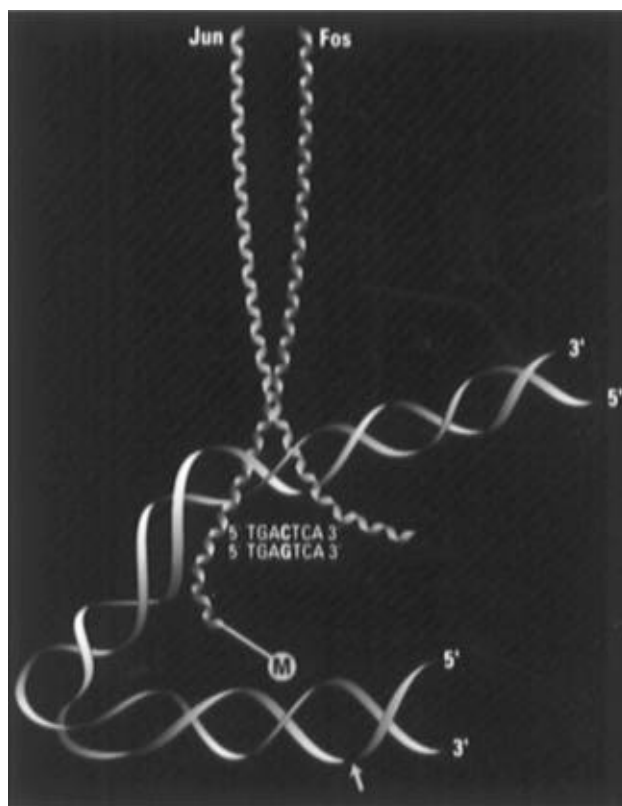


FIGURE 6: Diagram of DNA cleavage by M(II)-GKH-Fos(138–211). Jun(248–334) (blue) is shown complexed to M(II)-GKH-Fos(138–211) (red). Both are complexed to DNA (green). The metal (yellow) can be either Cu(II) or Ni(II). DNA cleavage occurs at 34–35 bp upstream on the 5' strand only when the AP-1 binding site is TGACTCA and 33 bp upstream on the 5' strand only when the AP-1 binding site is TGAGTCA. The break point on DNA with an arrow indicates DNA cleavage.

between the AP-1 binding site and the 33–35 bp region upstream from the site indicates that the DNA is bent by the binding of the two proteins so that the region which is slightly more than three turns upstream is brought back toward the AP-1 binding site. A composite model in Figure 6 shows the binding of M(II)-GKH-Fos(138–211) and Jun(248–334) heterodimers to DNA containing the AP-1 binding site and the DNA cleavage by the designed protein. This is consistent with the findings that Fos–Jun heterodimers bend DNA (Kerppola & Curran, 1991b). It has been demonstrated that Fos–Jun heterodimers of peptides encompassing only the DNA-binding and dimerization domains, i.e., Fos(116–211), Fos(139–211), Jun(224–334) and Jun(240–334), bend DNA by 57° toward the minor groove, resulting in bends of DNA toward the amino terminus of Fos (Kerppola & Curran, 1991b). Therefore, we have gained insight into the interaction between Fos and Jun and the bending of DNA by these two proteins.

## CONCLUSION

A protein has been designed which is capable of cleaving DNA. Once expressed, this protein retains the DNA-binding capabilities of its parent bZIP protein, Fos, as well as the

<sup>2</sup> A paper published after this paper was submitted demonstrated that the presence of positively charged residues in an ATCUN motif can increase DNA cleavage due to the increased affinity of the motif for the DNA phosphate backbone when compared to a GGH motif (Liang et al., 1995).

metal-binding properties of the ATCUN motif. The DNA-binding moiety brings the DNA cleavage moiety into close proximity to the DNA to increase the specificity of the DNA cleavage. These studies have demonstrated that the definition of the ATCUN motif (Predki et al., 1992) can be used to design proteins which have properties beyond the minimal GGH motif. The ATCUN motif therefore can be used to generate proteins which have properties due to (1) the metal-binding site, (2) the construct which is C-terminal to the tripeptide motif, and (3) the first two residues of the motif.<sup>2</sup> We therefore predict that many more protein designs can be accomplished using this motif.

## ACKNOWLEDGMENT

We are grateful to Dr. T. Curran for the gift of wbFos and wbJun, Drs. T. Kerppola and P. Lewis for helpful discussions, and Dr. P. F. Predki for the gift of p2R.

## REFERENCES

- Abate, C., Luk, D., Gentz, R., Rauscher, F. J., & Curran, T. (1990) *Proc. Natl. Acad. Sci. U.S.A.* 87, 1032–1036.
- Appleton, D. W., & Sarkar, B. (1971) *J. Biol. Chem.* 246, 5040–5046.
- Camerman, N., Camerman, A., & Sarkar, B. (1976) *Can. J. Chem.* 54, 1309–1316.
- Chiou, S. H. (1983) *J. Biochem. (Tokyo)* 94, 1259–1267.
- Curran, T. (1992) *Tohoku J. Exp. Med.* 168, 169–174.
- Dixon, J. W., & Sarkar, B. (1974) *J. Biol. Chem.* 249, 5872–5877.
- Fisher, D. E., Parent, L. A., & Sharp, P. A. (1992) *Proc. Natl. Acad. Sci. U.S.A.* 89, 11779–11783.
- Glennon, J. D., & Sarkar, B. (1982a) *Biochem. J.* 203, 15–23.
- Glennon, J. D., & Sarkar, B. (1982b) *Biochem. J.* 203, 25–31.
- Glennon, J. D., Hughes, D. W., & Sarkar, B. (1983) *J. Inorg. Biochem.* 19, 281–289.
- Glover, J. N. M., & Harrison, S. C. (1995) *Nature* 373, 257–261.
- Haber, F., & Weiss, J. J. (1934) *Proc. R. Soc. London, Ser. A* 147, 332–351.
- Hai, T., & Curran, T. (1991) *Proc. Natl. Acad. Sci. U.S.A.* 88, 3720–3724.
- Harford, C., & Sarkar, B. (1995) *Biochem. Biophys. Res. Commun.* 209, 877–882.
- Iyer, K. S. N., Lau, S., Laurie, S. H., & Sarkar, B. (1978) *Biochem. J.* 169, 61–69.
- Johnson, N. P., Lindstrom, J., Baase, W. A., & von Hippel, P. H. (1994) *Proc. Natl. Acad. Sci. U.S.A.* 91, 4840–4844.
- Kerppola, T., & Curran, T. (1991a) *Science* 254, 1210–1214.
- Kerppola, T., & Curran, T. (1991b) *Cell* 66, 317–326.
- Kimoto, E., Tanaka, H., Gyotoku, J., Morishige, F., & Pauling, L. (1983) *Cancer Res.* 43, 824–828.
- Klein, C. B., Frenkel, K., & Costa, M. (1991) *Chem. Res. Toxicol.* 4, 592–604.
- Kruck, T. P. A., Lau, S., & Sarkar, B. (1976) *Can. J. Chem.* 54, 1300–1308.
- Lau, S., & Sarkar, B. (1981) *J. Chem. Soc. Dalton Trans.* 491–494.
- Lau, S., Kruck, T. P. A., & Sarkar, B. (1974) *J. Biol. Chem.* 249, 5878–5884.
- Laussac, J.-P., & Sarkar, B. (1980a) *J. Biol. Chem.* 255, 7563–7568.
- Laussac, J.-P., & Sarkar, B. (1980b) *Can. J. Chem.* 58, 2055–2060.
- Laussac, J.-P., & Sarkar, B. (1984) *Biochemistry* 23, 2832–2838.
- Liang, Q., Eason, P. D., & Long, E. C. (1995) *J. Am. Chem. Soc.* 117, 9625–9631.
- Mack, D. P., & Dervan, P. B. (1990) *J. Am. Chem. Soc.* 112, 4604–4606.
- Mack, D. P., & Dervan, P. B. (1992) *Biochemistry* 31, 9399–9405.
- Mack, D. P., Iverson, B. L., & Dervan, P. B. (1988) *J. Am. Chem. Soc.* 110, 7572–7574.
- Nagaoka, M., Kuwahara, J., & Sugiura, Y. (1993) *Biochem. Biophys. Res. Commun.* 194, 1515–1520.
- Nagaoka, M., Hagihara, M., Kuwahara, J., & Sugiura, Y. (1994) *J. Am. Chem. Soc.* 116, 4085–4086.
- Patel, L. R., Curran, T., & Kerppola, T. K. (1994) *Proc. Natl. Acad. Sci. U.S.A.* 91, 7360–7364.
- Predki, P. F., & Sarkar, B. (1992) *J. Biol. Chem.* 267, 5842–5846.
- Predki, P. F., Harford, C., Brar, P., & Sarkar, B. (1992) *Biochem. J.* 287, 211–215.
- Sarkar, B. (1977) in *Metal Ligand Interaction in Organic Chemistry and Biochemistry* (Pullman, B., & Goldblum, N., Eds.) pp 193–228, D. Reidel Publishing Co., Dordrecht, Holland.
- Sarkar, B., Renugopalakrishnan, V., Kruck, T. P. A., & Lau, S. (1976) in *Environmental Effects on Molecular Structure and Properties* (Pullman, B., Ed.) pp 165–178, D. Reidel Publishing Co., Dordrecht, Holland.
- Sarkar, B., Dixon, H. B. F., & Webster, D. (1978) *Biochem. J.* 173, 895–897.
- Shriver, D. F., Atkins, P., & Langford, C. H. (1994) in *Inorganic Chemistry*, 2nd ed., pp 782–819, W. H. Freeman and Co., New York, NY.
- Shullenberger, D. F., Eason, P. D., & Long, E. C. (1993) *J. Am. Chem. Soc.* 115, 11038–11039.
- Tabata, M., & Sarkar, B. (1985a) *Can. J. Chem.* 63, 3111–3116.
- Tabata, M., & Sarkar, B. (1985b) *Can. J. Chem.* 63, 3117–3121.
- Tonetti, M., Giovine, M., Gasparini, A., Benatti, U., & De Flora, A. (1993) *Biochem. Pharmacol.* 46, 1377–1383.
- Torreilles, J., Guerin, M.-C., & Slaoui-Hasnaoui, A. (1990) *Free Radical Res. Commun.* 11, 159–166.
- Tullius, T. D. (1991) *Free Radical Res. Commun.* 12–13, 521–529.
- Xanthoudakis, S., & Curran, T. (1992) *EMBO J.* 11, 653–665.

BI9520186